

This is the peer reviewed version of the following article:

In hepatocellular carcinoma miR-221 modulates sorafenib resistance through inhibition of caspase-3-mediated apoptosis / Fornari, Francesca; Pollutri, Daniela; Patrizi, Clarissa; La Bella, Tiziana; Marinelli, Sara; Casadei Gardini, Andrea; Marisi, Giorgia; Baron Toaldo, M.; Baglioni, Michele; Salvatore, Veronica; Callegari, Elisa; Baldassarre, Maurizio; Galassi, Marzia; Giovannini, Catia; Cescon, Matteo; Ravaioli, Matteo; Negrini, Massimo; Bolondi, Luigi; Gramantieri, Laura. - In: CLINICAL CANCER RESEARCH. - ISSN 1557-3265. - 23:14(2017), pp. 3953-3965. [10.1158/1078-0432.CCR-16-1464]

Terms of use:

The terms and conditions for the reuse of this version of the manuscript are specified in the publishing policy. For all terms of use and more information see the publisher's website.

13/01/2026 02:16

In hepatocellular carcinoma miR-221 modulates Sorafenib resistance through inhibition of caspase-3 mediated apoptosis.

Francesca Fornari^{1,2}, Daniela Pollutri^{1*}, Clarissa Patrizi^{3*}, Tiziana La Bella^{4*}, Sara Marinelli¹, Andrea Casadei Gardini⁵, Giorgia Marisi⁶, Marco Baron Toaldo⁷, Michele Baglioni¹, Veronica Salvatore¹, Elisa Callegari⁸, Maurizio Baldassarre¹, Marzia Galassi¹, Catia Giovannini^{1,2}, Matteo Cescon⁹, Matteo Ravaoli⁹, Massimo Negrini⁷, Luigi Bolondi^{1,2}, Laura Gramantieri¹.

¹ Center for Applied Biomedical Research, St.Orsola-Malpighi University Hospital, 40138, Bologna, Italy.

² Department of Medical and Surgical Sciences, Bologna University, 40138, Bologna, Italy.

³ Center for Regenerative Medicine, Department of Biomedical Sciences, University of Modena and Reggio Emilia, 41125, Modena, Italy.

⁴ INSERM, UMR-1162, Functional Genomics of Solid Tumors, 75010, Paris, France.

⁵ Department of Medical Oncology, Istituto Scientifico Romagnolo per lo Studio e la Cura dei Tumori (IRST) IRCCS, 47014, Meldola, Italy.

⁶ Biosciences Laboratory, Istituto Scientifico Romagnolo per lo Studio e la Cura dei Tumori (IRST) IRCCS, 47014, Meldola, Italy.

⁷ Department of Veterinary Medical Sciences, Bologna University, 40064, Bologna, Italy.

⁸ Department of Morphology, Surgery and Experimental Medicine, Ferrara University, 44100, Ferrara, Italy.

⁹ Department of Medical and Surgical Sciences, General and Transplant Surgery Unit, St. Orsola-Malpighi University Hospital, 40138, Bologna, Italy.

* These Authors contributed equally to this work.

Running title: MiR-221 regulates Sorafenib response in HCC

Key words: HCC, microRNA, miR-221, Sorafenib, caspase.

Financial Support Statement:

1. Programma di Ricerca Regione-Università 2010-2012, Regione Emilia-Romagna, Bando "Ricerca Innovativa", to L.B. and L.G. "Innovative approaches to the diagnosis and

pharmacogenetic-based therapies of primary hepatic tumors, peripheral B and T-cell lymphomas and lymphoblastic leukaemias”.

2. Programma di Ricerca Regione-Università 2010-2012, Regione Emilia-Romagna, Bando "Alessandro Liberati", to F.F. "Identification of innovative microRNAs-based biomarkers and anti-cancer strategies for the treatment of Hepatocellular carcinoma”.

3. Italian Ministry of University and Research - PRIN 2010-2011 to L.B.

4. Fondazione del Monte in Bologna to L.G.

Corresponding Authors:

Laura Gramantieri, Francesca Fornari

Address: Via Massarenti, 9, 40138, Bologna, Italy.

Tel/Fax: +390512143902

E-mail: laura.gramantieri@aosp.bo.it, francesca.fornari2@unibo.it

Conflict of interest: The Authors have no conflict of interest to declare

Statement of translational relevance

A clinical challenge in the oncology field is represented by the identification of non-invasive biomarkers to be used for the prognostic stratification and for the personalization of treatments. Here we describe an association between miR-221 circulating levels and response to Sorafenib in animal models and in a preliminary cohort of patients with advanced HCC. Though preliminary, these findings identify a candidate biomarker of likelihood of response to Sorafenib to be validated in prospective clinical studies in HCC patients. Molecular events elucidating the mechanistic role of miR-221 changes in the modulation of response to Sorafenib are also provided.

Abstract

Purpose: The aberrant expression of miR-221 is a hallmark of human cancers, including hepatocellular carcinoma, and its involvement in drug resistance, together with a proved in vivo efficacy of anti-miR-221 molecules, strengthen its role as an attractive target candidate in the oncologic field. The discovery of biomarkers predicting the response to treatments represents a clinical challenge in the personalized treatment era. This study aimed to investigate the possible role of miR-221 as a circulating biomarker in HCC patients undergoing Sorafenib treatment as well as to evaluate its contribution to Sorafenib resistance in advanced HCC.

Experimental design: A chemically induced HCC rat model and a xenograft mouse model, together with HCC-derived cell lines were employed to analyze miR-221 modulation by Sorafenib treatment. Data from the functional analysis were validated in tissue samples from surgically resected HCCs. The variation of circulating miR-221 levels in relation to Sorafenib treatment were assayed in the animal models and in two independent cohorts of patients with advanced HCC.

Results: MiR-221 over-expression was associated with Sorafenib resistance in two HCC animal models and caspase-3 was identified as its target gene, driving miR-221 anti-apoptotic activity following Sorafenib administration. Lower pre-treatment miR-221 serum levels were found in patients subsequently experiencing response to Sorafenib and an increase of circulating miR-221 at the two months assessment was observed in responder patients.

Conclusions: MiR-221 might represent a candidate biomarker of likelihood of response to Sorafenib in HCC patients to be tested in future studies. Caspase-3 modulation by miR-221 participates to Sorafenib resistance.

Introduction

The up-regulation of miR-221 along with its oncogenic activity were previously reported in hepatocellular carcinoma (1-3), as well as in other cancers, such as glioblastoma (4, 5), papillary thyroid carcinoma (6, 7), pancreatic cancer (8), prostate (9), melanoma (10), breast (11), kidney and bladder cancer (12). Onco-miR-221 up-regulation can be considered a hallmark of cancer. We have also shown its tumor promoting functions in the liver of a miR-221 transgenic mouse, confirming its role as a therapeutic candidate (13).

Molecular mechanisms sustaining miR-221 oncogenic functions rely upon the regulation of cell proliferation (1) and impairment of apoptosis (3, 5). In addition, miR-221 plays an important role in the modulation of response to anti-cancer treatments through the regulation of key oncogenic factors such as the TP53-MDM2 axis (14), TIMP3 (15) and PTEN (16) molecules.

Even though Sorafenib represents the standard of care for advanced HCC and it is the only recommended treatment in this setting, there is no biomarker helpful in the prediction of sensitivity to this treatment. However, heterogeneous responses may be observed across patients treated by Sorafenib.

The discovery of novel target candidates increasing the efficacy of anti-cancer strategies and the identification of non-invasive biomarkers in liquid biopsies are two important clinical challenges in the oncologic field. It was widely demonstrated that microRNAs are optimal biomarkers due to their high stability in biologic fluids and the availability of easy detection methods (17, 18).

Here we explored, by using an *in vivo* and *in vitro* approach, the role of miR-221 as a tissue and circulating biomarker in the setting of Sorafenib treatment. To this aim, we employed two HCC models, a DEN induced HCC rat model and a xenograft mouse model, as well several HCC-derived cell lines. Moreover, we tested the circulating levels of miR-221 as a candidate non-invasive biomarker associated with response to Sorafenib treatment in advanced HCC, both in animal models and in a small and preliminary cohort of HCC patients. Finally, molecular mechanisms sustaining the role of miR-221 as an innovative therapeutic target in HCC were

investigated and caspase-3 modulation was assessed as a critical factor.

Patients and Methods

Patients

HCC and cirrhotic tissues were obtained from 60 randomly selected patients (45 males and 15 females, median age \pm SD: 70.0 \pm 8.5 years, range 49-82 years) undergoing liver resection for HCC. Tissues were collected at surgery and stored as previously described (19). Local ethics committee of St. Orsola-Malpighi University Hospital approved the study and all patients signed an informed consent. Histopathological grading was scored according to Edmondson and Steiner criteria (20). No patient received anticancer treatment prior to surgery. Antiviral treatment was administered to HBV-infected patients only. No HCV-infected patient received antiviral treatment except for interferon-based regimens performed at least three years before surgery. Eight normal liver tissues were obtained from patients undergoing liver surgery for traumatic lesions (5 cases) or haemangioma resection (3 cases). The characteristics of patients are detailed in Supplementary Table S1.

A further cohort of ninety-three patients with advanced HCC without extrahepatic metastases were tested for miR-221 circulating levels. Fifty patients from Bologna center (23 responders and 27 non-responders at 2 months) were tested before treatment start. Among these, 28 patients (12 responders and 16 non-responders) were assayed before treatment and at the two months assessment. The remaining forty-three patients (17 with stable disease and 26 patients with disease progression at 2 months) were tested for circulating miR-221 levels before treatment start (43 cases) and at the two months assessment (31 of 43 patients). These forty-three patients were enrolled by both the Bologna Center and the Department of Medical Oncology of Meldola's Center (Italy) and were considered as an independent validation cohort. Patients' characteristics are detailed in Supplementary Table S2 and Figure S1.

DEN-HCC rat model

Male Wistar rats (Harlan) received diethylnitrosamine (DEN, Sigma-Aldrich) in the drinking water (100 mg/l) for 8 weeks. Two weeks later the end of DEN treatment animals were weekly monitored by ultrasound imaging (US) (MyLab70 XVG, Esaote) (21). A first group of animals (N=18) was euthanized one or two months after the end of DEN treatment, when the major diameter of at least one HCC nodule reached a dimension of 10 mm at US. A second group of animals (N=10) received Sorafenib intragastrically for 21 days (10 mg/kg of body weight), starting when a 2-3 mm nodule was evident at US. Animals were segregated in responder and non responder groups according to US and histopathological examination. Two untreated animals were used as control. At sacrifice, HCC nodules and surrounding liver were collected for molecular biology and immunohistochemistry analyses. 23 and 16 HCC nodules were collected in the untreated and treated groups, respectively. At sacrifice, blood withdrawal was obtained from 13/18 untreated and 7/10 Sorafenib treated rats. Serum was achieved by centrifugation of blood samples at 4000 rpm for 10 min at 4°C. All animals received human care in accordance with the criteria published by the National Institutes of Health. Local ethics committee approved the research protocol (14/70/12).

HCC mice models

For the xenograft model, 3.0 million of Huh-7 cells were injected into both flanks of NOD/SCID (CB17PRKDC/J) female mice (N=15 animals). Four weeks following cell injection, tumor masses were weekly monitored by US examination and when the tumors reached a volume of about 40-50 mm³ (width x length x height/2) mice were randomized into two groups. One group (N=6) received intragastrically a dose of 60 mg/kg body weight of Sorafenib for 21 days, while the other group (N=9) received only the vehicle (75% water, 12.5% absolute ethanol and 12.5% Cremophor EL) (Sigma-Aldrich). Mice were euthanized one day after the end of the treatment or, in the case of the untreated group, when the tumor mass exceeded the volume of about 1 cm³. At sacrifice, tumor masses were collected for both molecular biology and histopathology

analyses. At sacrifice, blood withdrawal was obtained from all mice of the vehicle treated group and from 5/6 Sorafenib treated animals. Serum samples were obtained as above described. Local ethics committee approved the research protocol (23/79/14).

The miR-221 transgenic mouse model was performed as previously described (13, 14). Protein samples were extracted from liver tissues derived from 25 transgenic (TG) and 16 wild type (WT) animals. Ten TG mice were treated by hydrodynamic tail vein injection with anti-miR-221 oligonucleotides (300 µg/mouse) or with vehicle only (saline) for 48 hours. Four more animals were treated with anti-miR-221 oligonucleotides or with vehicle only in presence of Sorafenib treatment (intragastrical administration, 10 mg/kg) for 48 hours.

Cell culture and treatments

HepG2, Hep3B and PLC/PRF/5 cells were cultured with Eagles's Minimum Essential Medium while SNU398, SNU449, SNU182, SNU475 and Huh-7 were cultured with RPMI-1640 (Life Technologies). Media were supplemented with 10% FBS, 2 mM L-Glutamine and 1X Penicillin/Streptomycin (Life Technologies). All the cell lines, except Huh-7, were purchased from ATCC. Huh-7 cells are from Prof. Alberti's laboratory, University of Padua, Italy. Cell clones used for experiments were previously authenticated. Cells were treated with 5.0 µM Sorafenib-tosylate (Bayer) for 48 hours. All experiments were performed in triplicate.

Cells were also treated with 1.0 µM of PI3K α/δ inhibitor (GDC-0941), Raf inhibitor (PLX-4720) and VEGFR2 inhibitor (ZM323881) for 48 hours (Selleckchem).

Cell transfection

HCC cells were transfected with 100 nM of pre-miR-221, anti-miR-221, or Negative Control#1 precursor and inhibitor miRNAs (Ambion). BMF and caspase-3 small interfering RNA pools (Trifecta RNAi Kit, IDT) were used at a concentration of 20 nM for 24 and 48 hours.

Oligonucleotide transfection was performed by using Lipofectamine 2000 (Life Technologies) according to manufacturer's instructions.

Stable transfection

For miR-221 over-expression in Huh-7 cells, the DNA sequence of mature miR-221 was inserted into the pGFP-V-RS retroviral vector (OriGene Technologies). The cells were infected and selected as previously described (14).

Luciferase activity assay

The 3'UTR region of human CASP3 gene was amplified by PCR using primers and conditions reported in Supplementary Table S3. Luciferase reporter assay of pGL3 3'UTR-containing vector was performed in HepG2 and SNU449 cells as previously reported (22).

Caspase 3/7 activity assay and viability assay

Apoptosis activation and cell viability were evaluated in Sorafenib treated HCC cells by using Caspase-Glo 3/7 and Cell-titer-Glo assays (Promega) according to manufacturers' instructions. Each sample was analyzed in quadruplicate.

Real-time PCR and RT-PCR

MiRNA-221-3p expression in HCC cells and tissue samples was evaluated by TaqMan MicroRNA Assay (ID: 000524) (Applied Biosystems), as previously described (19). RNU6B (ID: 001093) was used as housekeeping gene for human samples, whereas 4.5S RNA(H) (ID: 001717) and snoRNA412 (ID: 001243) were used for samples of rat and mouse origin, respectively. A pool of RNAs from two HCC cell lines or two HCC rat livers or two mouse

livers was used as reference sample for the $2^{-\Delta\Delta C_t}$ method for the quantification of samples of human or rat or mouse origin, respectively.

CASP3, *BMF*, *AFP*, *EpCAM*, *CK19* and *MYC* mRNAs was quantified by both semi-quantitative PCR and SYBR-green (Bio-Rad Laboratories) Real-time PCR analyses. β -actin expression was considered for gene normalization. Real-Time PCR experiments were run in triplicate. Primers and conditions are detailed in Supplementary Table S4.

Serum and exosome miRNA extraction

Isolation of circulating miRNAs from exosomes and cell culture supernatant of untreated and Sorafenib treated HCC cells was executed by an ultracentrifugation-based protocol as previously reported (23). Total RNA was isolated from 200 μ l of serum, cell culture supernatant, exosomes enriched or depleted fractions by using MiRNeasy Serum/Plasma Kit (Qiagen). Briefly, 12.5 fmol of a synthetic RNA corresponding to cel-miR-39 sequence (Ambion) were added to each sample after Qiazol addition. RNA was suspended in 35 μ l of DEPC water and used at a 1:3 dilution for qPCR quantification of miR-221 and cel-miR-39.

Western Blot

Thirty micrograms of whole protein extracts from cells and tissues were subjected to vertical electrophoresis, transferred to a nitrocellulose membrane (GE Healthcare) and assayed with antibodies reported in Supplementary Table S5. Digital images of X-ray films were quantified by ChemiDocTM XRS+ (Image LabTM Software, Bio-Rad). Western blot analysis was performed in triplicate.

Flow cytometry analysis

Transfected HCC cells were treated with 5 μ M Sorafenib for 48 hours. Detection of apoptotic cells was performed in triplicate by flow cytometry (FACSaria cell sorter, BD Biosciences) with Annexin V/Propidium Iodide detection kit (Bender MedSystems).

Statistical analysis

Differences between groups were analyzed using paired or unpaired Student's t-test, for in vitro assays and for the analysis of HCC-related variables, including miR-221 and caspase-3 expression in primary tumors as well as circulating miR-221 levels. Pearson's correlation coefficient was used to explore relationships between two variables. In vitro experiments were performed in triplicate and the mean values were used for the statistical analysis. Reported p-values were two-sided and considered significant when lower than 0.05. Statistical calculations were executed using SPSS version 15.0 (SPSS inc). * $p < 0.05$, ** $p < 0.01$, *** $p < 0.001$.

Results

High intra-tumor miR-221 levels are associated with Sorafenib resistance in HCC animal models

The role of onco-miR-221 in hepatocarcinogenesis (13, 19, 24) and response to treatments in HCC is documented (14-16). Here we employed two HCC animal models to investigate miR-221 involvement in Sorafenib resistance.

The first animal model is a chemically-induced HCC rat model displaying miR-221 over-expression in tumor tissue in 65% of cases, with a mean increase of 2.8-fold in HCC nodules (N=23) when compared to matched surrounding liver (N=16) (**Figure 1A**). Notably, miR-221 deregulated expression observed in this model reflects findings reported in human HCC (19). Moreover, the non-neoplastic liver tissue of DEN-treated animals displays no difference in miR-221 expression when compared to healthy control rats, ruling out miR-221 modulation by DEN.

Following Sorafenib administration, HCC nodules (N=16) were considered as responders or non-responders, based on US monitoring performed weekly during the follow-up after DEN discontinuation and histopathological examination at sacrifice (**Figure S2**). QPCR analysis showed higher intra-tumor miR-221 levels in non-responder versus responder rat HCCs (Student's t-test: $p=0.0013$; **Figure 1B**), suggesting that miR-221 might be implicated in Sorafenib resistance. To characterize if Sorafenib resistance might be related to the expression of specific oncogenes, *AFP*, *EPCAM*, *CK19* and *MYC* mRNA levels were analyzed in treated HCC animals. Higher *EPCAM* mRNA were detected in HCC nodules non-responding to Sorafenib with respect to the responder group (Student's t-test: $p=0.0011$; **Figure 1C**), while no difference was detected for *AFP*, *CK19* and *MYC* expression (**Figure S3A, B, C**).

The second animal model was a xenograft mouse model obtained by subcutaneous injection of Huh-7 cells into animal flanks. This model was chosen because it displays a relevant response to Sorafenib treatment, which is easily assessable by US examination (25). In this model, Sorafenib

administration determined a reduction of tumor size of 3.5-folds with respect to vehicle-treated mice (mean \pm SD: 238 \pm 119 vs 836 \pm 490 mm³; Student's t-test: p=0.0062; **Figure 1D**). Similarly, a 1.6-fold increase in tumor doubling time was observed in Sorafenib treated mice in comparison with controls (mean \pm SD: 4.3 \pm 2.0 vs 6.9 \pm 0.9 mm³; Student's t-test, p=0.0044; **Fig. 1E**). An inverse correlation was found between tumor size and tumor doubling time (Pearson's correlation, p=0.002; **Figure S3D**).

When miR-221 levels were assessed in the tumor masses from untreated animals, no correlation was found with respect to size and tumor doubling time. Conversely, in Sorafenib-treated mice a positive correlation was detected between miR-221 expression and tumor size (Pearson's correlation: R=0.66; p=0.048; **Figure 1F**), letting us to hypothesize that also in this model high miR-221 levels might be associated with Sorafenib resistance.

Circulating miR-221 levels predict response to Sorafenib

Since higher miR-221 tissue levels are associated with Sorafenib resistance in the rat HCC model and with increased tumor mass in the xenograft model, we investigated the relationships between tissue and circulating miR-221 levels in these models, to define its role as a possible circulating biomarker.

MiR-221 expression was quantified in serum samples and tumor tissues from 13 DEN-HCC untreated rats. As shown in **Figure 2A**, a correlation was found between miR-221 levels in HCC tissue and serum samples (Pearson's correlation: R=0.58; p=0.045). Only the larger nodule was considered in animals bearing more than one HCC, hypothesizing that it might be the main source of miRNAs release into the bloodstream. When considering more nodules in rats with a multinodular HCC, a positive correlation, even though not statistically significant, was confirmed between tissue and circulating miR-221 levels (Pearson's correlation: R=0.42; p=0.087) (**Figure S3E**).

These findings were confirmed in the mouse model displaying a correlation between circulating and intra-tumor miR-221 levels in untreated animals (Pearson's correlation: $R=0.66$; $p=0.048$; **Figure 2B**).

Subsequently, we tested circulating miR-221 levels in the setting of Sorafenib treatment in both models. Sorafenib treated DEN-HCC rats displayed an inverse correlation between circulating and tissue miR-221 levels (Pearson's correlation: $R=-0.75$; $p=0.050$; **Figure 2C**). This finding suggests that Sorafenib might have a role in miR-221 release from neoplastic hepatocytes into the bloodstream. The same result was confirmed in the mouse model, displaying a negative correlation between circulating miR-221 levels and both tissue miR-221 levels (Pearson's correlation: $R=-0.88$; $p=0.047$) and tumor size (Pearson's correlation: $R=-0.96$; $p=0.003$; **Figure 2D, 2E**).

We next explored the mechanisms contributing to miR-221 release into the bloodstream in basal conditions as well as following Sorafenib. Eight HCC-derived cell lines were assayed and a correlation between miR-221 levels in cell culture supernatant and exosome fraction was found, suggesting exosome vesicles as a source of circulating miR-221 (Pearson's correlation: $R=0.928$; $p=0.001$), as previously demonstrated by us in HCC patients (23).

In HCC cells, Sorafenib increased miR-221 levels in cell culture supernatant (Student's t-test: $p=0.01$; **Figure 2F**), as well as in its exosomal fraction (Student's t-test: $p=0.009$; **Figure 2G**) while miR-221 levels decreased in the intracellular compartment (Student's t-test: $p=0.02$; **Figure 2H**). These findings suggest a direct role of Sorafenib in the variation of miR-221 expression in both the intracellular and extracellular compartments in HCC. To evaluate which molecular pathway modulated by Sorafenib was mainly involved in miR-221 secretion from the intra to the extracellular compartment, we tested eight HCC-derived cell lines with three inhibitors of molecular pathways modulated by Sorafenib (PLX-4720 inhibiting BRAF, RAF1 and CRAF; ZM323881 inhibiting VEGFR2; GDC-0941 inhibiting PI3K α/δ). We compared miR-

221 changes in the extracellular compartments in treated versus untreated cells. PLX-4720 administration, inhibiting the Ras/Raf/Mek/Erk pathway, determined an increase in miR-221 extracellular levels in SNU475 cells only, while no relevant increase was detected in the other cell lines. Similarly, no significant increase was observed following VEGFR2 inhibition, obtained by ZM323881 administration, in all the cell lines. The inhibition of PI3K α/δ was performed due to the relevant role of pAKT in exosomal trafficking in cancer cells. Since a high heterogeneity was found in constitutive activation of MAPK and PI3K-Akt pathways, HCC-derived cell lines were evaluated taking into account basal expression levels of each pathway and the extent of miR-221 variations following treatments. Sorafenib administration determined miR-221 extrusion from the intra to the extracellular compartment in HepG2 (with the most relevant effect), Hep3B, Huh-7, SNU398, SNU182 and PLC cells, but no in SNU475 and SNU449 cells. Notably, following Sorafenib treatment, an opposite phosphorylation pattern of Akt was observed in HepG2 versus SNU449 and SNU475 cells. Therefore, we hypothesized that pAkt levels might be relevant as far as miR-221 release from HCC cells is concerned (**Figure 2I**). A relevant increase of miR-221 extracellular levels was observed by PI3K inhibition in SNU449 and SNU475 cells. The effects on miR-221 extrusion in HepG2, SNU449 and SNU475 cells treated by Sorafenib was thus opposite to what observed following GDC-0941. GDC-0941 treatment was not able to reduce pAkt levels in HepG2 cells where no variation of miR-221 extracellular levels was detected, whereas it reduced pAkt levels in SNU449 and SNU475 cells where an increase of miR-221 extrusion was detected (**Figure 2L**). Thus, we can speculate that the inhibition of the PI3K-pAkt axis by GCD-0941 might be responsible for miR-221 extrusion in these cells. Notably, the extent of Sorafenib treatment in miR-221 secretion is higher than that observed after PI3K inhibition, thus supporting the contribution of other molecular events.

High circulating miR-221 levels are associated with response to Sorafenib in HCC patients.

As described above, both rodent models suggested that higher miR-221 tissue levels were associated with Sorafenib resistance. Conversely, higher circulating miR-221 levels correlated with smaller tumor size, and inversely correlated with tissue miRNA levels. These findings prompted us to assay circulating miR-221 levels in Sorafenib-treated HCC patients.

To test miR-221 as a possible circulating biomarker predicting the likelihood of response to Sorafenib, we analyzed miR-221 levels in sera from HCC patients before Sorafenib treatment. Patients experiencing radiologic disease progression (N=27) showed higher pre-treatment miR-221 levels when compared with responders (N=23), as assessed at 2 months CT/MR examination (t-test: $p=0.007$; **Figure 3A**). Among the fifty patients tested before treatment start, 28 patients (12 responders and 16 non-responders) were further tested at 2 months follow-up. When comparing pre-treatment and on-treatment miR-221 levels in the same patient, an increase of miR-221 levels was detected in responders (paired t-test: $p=0.042$; **Figure 3B**), whereas a non-significant decrease of miR-221 levels was registered in non-responders (paired t-test: $p=0.058$).

An independent small validation cohort of 43 advanced HCC patients enrolled by the Department of Medical Oncology of the Meldola's Cancer Center and by the Bologna's Center was assessed for circulating miR-221 before treatment start and at the two months follow-up in 31 of 43 patients. Even though the number of patients included is too small to draw any conclusion, this validation series confirmed the findings obtained in the training set, as shown in **Figure 3C**. The 26 patients experiencing a partial response or disease progression at two months displayed higher miR-221 serum levels when compared with the 17 patients with a stable disease (t-test, $p=0.04$). Among the 17 responders, 14 patients were assessed also at the two months follow-up and an increase of miR-221 circulating levels was confirmed when compared with miR-221 pre-treatment levels (paired t-test test, $p=0.05$). As observed in the training set, a non-significant reduction of miR-221 serum levels at the two months follow-up was observed in 17 of 26 tested non-responder patients (paired t-test, $p=0.07$). In conclusion, lower pre-treatment miR-221 serum levels are associated with response to Sorafenib. In addition, treatment response

was associated with an increase of circulating miR-221, suggesting a possible secretion of this onco-miRNA from the intracellular compartment of neoplastic cells.

MiR-221 decreases apoptosis in Sorafenib-treated HCC cell lines

To study miR-221 involvement as a possible contributor to Sorafenib resistance, HCC-derived cells were transfected with pre or anti-miR-221 and treated with Sorafenib for 48 hours.

Specifically, we chose Huh-7 and Hep3B cells for miR-221 over-expression because of their low miR-221 basal levels, while miR-221 silencing was performed in SNU449 and SNU182 cells due to their high miR-221 basal levels, as previously reported (14). Transient miR-221 over-expression in Sorafenib-treated Huh-7 and Hep3B cells increased cell viability (Student's t-test: $p=0.04$ and $p=0.017$, respectively) and decreased caspase 3/7 activity (Student's t-test: $p=0.006$ and $p=0.033$, respectively) and expression (**Figure 4A, B**). A similar effect was observed in Huh-7 cells stably over-expressing miR-221, indicating that even a low miR-221 increase (6.5-fold) is sufficient to reduce Sorafenib anti-cancer activity (Student's t-test: $p=0.0008$ and $p=0.002$ for cell viability and caspase assay, respectively; **Figure 4C**). Conversely, miR-221 silencing in Sorafenib-treated SNU182 and SNU449 cells decreased cell viability (Student's t-test: $p=0.03$ and 0.001 , respectively) and increased caspase 3/7 activity (Student's t-test: $p=0.003$ and 0.016 , respectively) and expression (**Figure 4D, E**). Notably, miR-221 did not alter Bax and Puma protein expression in all the cell lines except Hep3B, (**Figure 4A-E**), suggesting a main involvement of the caspase cascade in miR-221-mediated Sorafenib resistance. FACS-Anexin V assay performed in stably over-expressing miR-221 Huh-7 cells following Sorafenib challenge further confirmed these data. A 1.4-fold decrease of events in late apoptosis was detected in miR-221 over-expressing cells (Student's t-test: $p=0.01$) (**Figure 4F**). These data highlighted an involvement of miR-221 in Sorafenib resistance of HCC cells, associated with inhibition of the caspase signaling.

MiR-221 targets caspase-3 in HCC cell lines

To clarify mechanisms sustaining miR-221 involvement in Sorafenib resistance, a computational analysis was performed identifying *CASP3* (NM_004346) among its target genes (TargetScan and MiRanda algorithms; **Figure 5A**). To identify the best in vitro models to study caspase-3 regulation by miR-221, their expression levels were assayed in HCC-derived cell lines. An inverse correlation was found between miR-221 and caspase-3 mRNA and protein levels (Spearman's correlation $p=0.036$; **Figure 5B**).

The functional analysis was performed based on miR-221 basal levels in HCC cells. HepG2 and Huh-7 cells were chosen for miR-221 over-expression whereas SNU449 and SNU182 cells were selected for miR-221 silencing. Cell transfection of pre-miR-221 in HepG2 and Huh-7 cells reduced caspase-3 expression at both protein and mRNA levels. The same was confirmed in Huh-7 cells stably over-expressing miR-221, by retroviral infection (**Figure 5C-E**). Conversely, anti-miR-221 transfection in SNU449 and SNU182 cells increased both caspase-3 mRNA and protein expression (**Figure 5F-G**). To prove a direct interaction between miR-221 and its target gene, the 3'UTR region of caspase-3 mRNA was cloned downstream a reporter gene and the resulting vector (pGL3-casp-3) was employed in a dual-luciferase assay. Co-transfection of pGL3-casp-3 vector with miR-221 in HepG2 cells or with AM-221 in SNU449 cells caused a 1.5-fold decrease and a 1.6-fold increase of the luciferase activity, respectively (Student's t-test: $p=0.007$ and $p=0.001$, respectively; **Figure 5H**). Finally, to demonstrate that caspase-3 targeting is an important mechanism mediating Sorafenib resistance by miR-221, SNU449 cells were co-transfected with anti-miR-221 oligonucleotides and caspase-3 siRNAs and subsequently treated with Sorafenib. WB analysis showed that caspase-3 inhibition was able to counteract the activation of the caspase cascade triggered by miR-221 silencing, decreasing the levels of cleaved fractions of caspase-3, caspase-7 and PARP, with respect to anti-miR-221 only

transfected cells (**Figure 5I**). These data demonstrated that miR-221 directly modulates caspase-3 expression in HCC cells by mRNA degradation and that caspase-3 targeting is involved, at least in part, in miR-221-mediated Sorafenib resistance.

MiR-221 regulates caspase-3 expression in vivo

To confirm the regulation of caspase-3 by miR-221, a liver-specific miR-221 transgenic (TG) mouse model (13) was employed. Caspase-3 protein levels were quantified by WB analysis in liver samples from 25 TG and 16 wild type (WT) animals. A 1.4-fold decrease of caspase-3 expression was observed in TG mice with respect to WT controls (Student's t-test: $p=0.022$; **Figure 6A, B**). Moreover, to demonstrate that miR-221 was able to regulate caspase-3 expression *in vivo*, we performed miR-221 silencing in this TG mouse model by means of chemically-modified oligonucleotides (13). A mean 2.0-fold increase of caspase-3 protein levels was detected in liver tissue of antimiR-221-treated mice with respect to control group (**Figure 6C**). Furthermore, we observed that caspase-3 upregulation was maintained in antimiR-221-treated animals also following Sorafenib administration in comparison to vehicle-treated mice. *In vivo* miR-221 silencing was verified in both settings by QPCR analysis (**Figure 6D**). These findings proved the caspase-3 targeting by miR-221 *in vivo* and suggested that this molecular mechanism might contribute to Sorafenib resistance in miR-221 overexpressing HCCs.

MiR-221 and caspase-3 correlation was also investigated in the tumor tissue from the DEN-induced HCC rat model. As reported in **Figure 1A**, when comparing HCC versus its matched surrounding liver tissue, miR-221 expression increased in 65% of HCC tissues while caspase-3 mRNA and protein levels decreased in 70% and 50% of HCC nodules, respectively. An inverse correlation between miR-221 and caspase-3 was observed at both mRNA and protein levels in rat HCCs (Pearson's correlation: $p=0.009$ and $p=0.04$, respectively; **Figure 6E, F, S3F**). We

previously demonstrated that miR-221 regulates apoptosis through Bmf targeting (3). Here we confirm an inverse correlation between miR-221 and Bmf mRNA (Pearson's correlation: $R=-0.53$, $p=0.008$) and a positive correlation between Bmf and caspase-3 mRNA (Pearson's correlation: $R=0.71$, $p<0.0001$) in rat HCCs, suggesting that miR-221 regulates apoptosis through a multi-target activity (**Figure S3G, H**). In vitro experiments confirmed the ability of miR-221 to target contemporaneously caspase-3 and Bmf proteins in transfected HepG2 and SNU449 cells. Moreover, the silencing of caspase-3 slightly decreased Bmf protein levels (**Figure S3I**), letting us to hypothesize a complex interplay among miR-221 and these two pro-apoptotic targets.

Finally, we investigated the relationship between miR-221 and caspase-3 levels in 60 patients surgically resected for HCC. An inverse correlation between miR-221 and its target gene is shown in **Figure 6G** (Pearson's correlation: $R=-0.45$, $p<0.0001$). In line with the HCC rat model, a mean 3.0-fold increase of miR-221 levels was detected in HCC samples with respect to matched cirrhotic livers, whereas similar miR-221 levels were quantified in normal livers and non-tumor samples. In addition, comparable miR-221 levels were observed in HCC patients and HCC cell lines with low basal levels (HepG2, Hep3B and Huh-7) (**Figure S3L**). As previously reported, high miR-221 levels were associated with HCC multifocality (Student's t-test, $p=0.013$; **Figure 6H**) (3). Here, we also report an association between reduced caspase-3 expression and HCC multifocality (Student's t-test, $p=0.02$; **Figure 6I**). Moreover, we investigated the possible associations between miR-221 and caspase-3 expression and tumor characteristics. No association between miR-221 or caspase-3 mRNA levels and clinicopathologic features (AFP serum levels, tumor size, etiology and grading) was detected in this cohort of surgically resected patients (**Figure S4**). These data confirm that miR-221 and caspase-3 aberrant expression in HCC is associated with tumor multi-nodularity but is independent from other clinical variables.

Discussion

The oncogenic function of miR-221 in hepatocarcinogenesis is well documented (13, 19, 24). Similarly, its role in the regulation of cell proliferation, apoptosis (1, 3, 5) and treatment resistance (14-16) was previously ascertained. In an orthotopic mouse model of HCC, Park demonstrated the therapeutic efficacy of miR-221 inhibition, suggesting miR-221 as a target in patients with HCC (26). These findings were confirmed in our transgenic HCC mouse model, in which anti-miR-221 systemic treatment reduced number and size of HCC nodules (13).

MiRNAs modulation triggered significant effects in the response to anticancer treatments in different cancers. Specifically, miR-221 over-expression in HER-2-positive breast cancer cells inhibited apoptosis and promoted metastasis and trastuzumab resistance by targeting *PTEN*. This study suggested a role of miR-221 as a potential biomarker for the assessment of progression and poor prognosis, as well as a novel target for trastuzumab-combined treatment for HER2-positive breast cancer (27). Similarly, miR-221 silencing sensitized HCC and NSCLC cells to TRAIL by regulating *PTEN* and *TIMP3* (16). A recent study reported miR-221 involvement in dexamethasone resistance through *PUMA* down-regulation in multiple myeloma suggesting miR-221 as a marker of prognosis and clinical response in this context (28). Here we report miR-221 over-expression in HCC tissue as a molecular event associated with resistance to Sorafenib in two HCC animal models. In particular, in the chemically-induced HCC rat model an association between high miR-221 intra-tumor levels and Sorafenib resistance was observed, whereas in the xenograft mouse model a direct correlation between miR-221 levels and tumor size was registered. We also demonstrated that caspase-3 is a direct target of miR-221 in HCC, further suggesting miR-221 inhibition as a therapeutic approach aimed to contrast resistance to Sorafenib. A recent study describes an inverse correlation between caspase-3 and miR-221 in several cancer cell lines (29), but no clear evidence of a direct targeting was provided. Therefore,

to our knowledge, this is the first time that caspase-3 is shown to be directly modulated by miR-221 in HCC. Moreover, here we showed a complex regulatory network between miR-221 and its two pro-apoptotic targets, caspase-3 and Bmf. Indeed, we confirmed our previous findings (3) reporting a mutual regulation between Bmf and caspase-3 expression and activation in in vitro models and we identified a positive correlation between them in preclinical animal models. We might speculate that both targets are important for miR-221 biological activity and that the prevalence of one of them might be dependent on cell context, basal levels and type of apoptotic stimuli.

A clinical challenge in the oncology field is represented by the identification of non-invasive biomarkers to be used for the prognostic stratification and for the personalization of treatments. Here we describe an association between miR-221 circulating levels and response to Sorafenib in animal models and in patients with advanced HCC undergoing Sorafenib treatment. An inverse correlation between miR-221 serum levels (at the end of treatment) and tumor size was detected in treated animals, letting us to hypothesize low miR-221 circulating levels as a possible biomarker of Sorafenib resistance. In HCC patients, Sorafenib treatment determined an increase of miR-221 circulating levels only in responders. Conversely, before Sorafenib start, lower miR-221 circulating levels, assessed at baseline, were associated with response to treatment. Even though the patients cohorts tested here are too small to draw any conclusion, circulating miR-221 might deserve attention as a candidate non invasive biomarker of response to Sorafenib to be tested in prospective trials.

Since Sorafenib treatment influences miR-221 intratumoral and circulating levels, we next investigated the mechanisms sustaining miR-221 secretion from neoplastic cells, by exploring the effects of Sorafenib in HCC-derived cell lines. Sorafenib administration determined the extrusion of miR-221 from HCC cells into cell culture supernatant in an exosome-dependent manner, determining a reduction of its intracellular levels. Since several pro-apoptotic factors, such as *BMF*, *BIM* and *PUMA*, are miR-221 targets (3, 30, 31), the secretion of this oncomiRNA

in the extracellular compartment might decrease its intra-cytoplasmic levels, thus reducing its anti-apoptotic activity and sensitizing HCC cells to Sorafenib. These events were demonstrated in HCC cells and we can hypothesize that a similar mechanism might occur in primary tumors, even though we cannot exclude that the tumor surrounding tissue or tumor infiltrating cells can contribute to miR-221 release into the bloodstream. Despite we cannot provide a direct demonstration of miR-221 provenience, findings obtained from two animal models, cell lines and a restricted series of patients with advanced HCC are consistent with its role as a candidate biomarker of likelihood of response to Sorafenib, as well as a non-invasive and dynamic assay to be validated in prospective clinical studies in HCC patients.

References

1. Fornari F, Gramantieri L, Ferracin M, Veronese A, Sabbioni S, Calin GA, et al. MiR-221 controls CDKN1C/p57 and CDKN1B/p27 expression in human hepatocellular carcinoma. *Oncogene* 2008;27:5651-61.
2. Gramantieri L, Fornari F, Callegari E, Sabbioni S, Lanza G, Croce CM, et al. MicroRNA involvement in hepatocellular carcinoma. *J Cell Mol Med* 2008;12:2189-204.
3. Gramantieri L, Fornari F, Ferracin M, Veronese A, Sabbioni S, Calin GA, et al. MicroRNA-221 targets Bmf in hepatocellular carcinoma and correlates with tumor multifocality. *Clin Cancer Res* 2009;15:5073-81.
4. Ciafre SA, Galardi S, Mangiola A, Ferracin M, Liu CG, Sabatino G, et al. Extensive modulation of a set of microRNAs in primary glioblastoma. *Biochem Biophys Res Commun* 2005;334:1351-58.
5. Zhang CZ, Zhang JX, Zhang AL, Shi ZD, Han L, Jia ZF, et al. MiR-221 and miR-222 target PUMA to induce cell survival in glioblastoma. *Mol Cancer* 2010;9:229.
6. He H, Jazdzewski K, Li W, Liyanarachchi S, Nagy R, Volinia S, et al. The role of microRNA genes in papillary thyroid carcinoma. *Proc Natl Acad Sci U S A* 2005;102:19075-80.
7. Pallante P, Visone R, Ferracin M, Ferraro A, Berlingieri MT, Troncone G, et al. MicroRNA deregulation in human thyroid papillary carcinomas. *Endocr Relat Cancer* 2006;13:497-508.
8. Lee EJ, Gusev Y, Jiang J, Nuovo GJ, Lerner MR, Frankel WL, et al. Expression profiling identifies microRNA signature in pancreatic cancer. *Int J Cancer* 2007;120:1046-54.
9. Galardi S, Mercatelli N, Giorda E, Massalini S, Frajese GV, Ciafre SA, et al. miR-221 and miR-222 expression affects the proliferation potential of human prostate carcinoma cell lines by targeting p27Kip1. *J Biol Chem* 2007;282:23716-24.
10. Felicetti F, Errico MC, Bottero L, Segnalini P, Stoppacciaro A, Biffoni M, et al. The promyelocytic leukemia zinc finger-microRNA-221/-222 pathway controls melanoma progression through multiple oncogenic mechanisms. *Cancer Res* 2008;68:2745-54.
11. Rao X, Di Leva G, Li M, Fang F, Devlin C, Hartman-Frey C, et al. MicroRNA-221/222 confers breast cancer fulvestrant resistance by regulating multiple signaling pathways. *Oncogene* 2011;30:1082-97.
12. Gottardo F, Liu CG, Ferracin M, Calin GA, Fassan M, Bassi P, et al. Micro-RNA profiling in kidney and bladder cancers. *Urol Oncol* 2007;25:387-92.

13. Callegari E, Elamin BK, Giannone F, Milazzo M, Altavilla G, Fornari F, et al. Liver tumorigenicity promoted by microRNA-221 in a mouse transgenic model. *Hepatology* 2012;56:1025-33.
14. Fornari F, Milazzo M, Galassi M, Callegari E, Veronese A, Miyaaki H, et al. p53/mdm2 feedback loop sustains miR-221 expression and dictates the response to anticancer treatments in hepatocellular carcinoma. *Mol Cancer Res* 2014;12:203-16.
15. Gan R, Yang Y, Yang X, Zhao L, Lu J, Meng QH. Downregulation of miR-221/222 enhances sensitivity of breast cancer cells to tamoxifen through upregulation of TIMP3. *Cancer Gene Ther* 2014;21:290-96.
16. Garofalo M, Di Leva G, Romano G, Nuovo G, Suh SS, Ngankea A, et al. miR-221&222 regulate TRAIL resistance and enhance tumorigenicity through PTEN and TIMP3 downregulation. *Cancer Cell* 2009;16:498-509.
17. Mitchell PS, Parkin RK, Kroh EM, Fritz BR, Wyman SK, Pogosova-Agadjanyan EL, et al. Circulating microRNAs as stable blood-based markers for cancer detection. *Proc Natl Acad Sci U S A* 2008;105:10513-18.
18. Ferracin M, Lupini L, Salamon I, Saccenti E, Zanzi MV, Rocchi A, et al. Absolute quantification of cell-free microRNAs in cancer patients. *Oncotarget* 2015;6:14545-55.
19. Gramantieri L, Ferracin M, Fornari F, Veronese A, Sabbioni S, Liu CG, et al. Cyclin G1 is a target of miR-122a, a microRNA frequently down-regulated in human hepatocellular carcinoma. *Cancer Res* 2007;67:6092-99.
20. Edmondson HA, Steiner PE. Primary carcinoma of the liver: a study of 100 cases among 48,900 necropsies. *Cancer* 1954;7:462-503.
21. Giovannini C, Minguzzi M, Baglioni M, Fornari F, Giannone F, Ravaioli M, et al. Suppression of p53 by Notch3 is mediated by Cyclin G1 and sustained by MDM2 and miR-221 axis in hepatocellular carcinoma. *Oncotarget* 2014;5:10607-20.
22. Fornari F, Gramantieri L, Giovannini C, Veronese A, Ferracin M, Sabbioni S, et al. MiR-122/cyclin G1 interaction modulates p53 activity and affects doxorubicin sensitivity of human hepatocarcinoma cells. *Cancer Res* 2009;69:5761-67.
23. Fornari F, Ferracin M, Trere D, Milazzo M, Marinelli S, Galassi M, et al. Circulating microRNAs, miR-939, miR-595, miR-519d and miR-494, Identify Cirrhotic Patients with HCC. *PLoS One* 2015;10:e0141448.
24. Pineau P, Volinia S, McJunkin K, Marchio A, Battiston C, Terris B, et al. miR-221 overexpression contributes to liver tumorigenesis. *Proc Natl Acad Sci U S A* 2010;107:264-69.

25. Baron Toaldo M, Salvatore V, Marinelli S, Palama C, Milazzo M, Croci L, et al. Use of VEGFR-2 targeted ultrasound contrast agent for the early evaluation of response to sorafenib in a mouse model of hepatocellular carcinoma. *Mol Imaging Biol* 2015;17:29-37.
26. Park JK, Kogure T, Nuovo GJ, Jiang J, He L, Kim JH, et al. miR-221 silencing blocks hepatocellular carcinoma and promotes survival. *Cancer Res* 2011;71:7608-16.
27. Ye X, Bai W, Zhu H, Zhang X, Chen Y, Wang L, et al. MiR-221 promotes trastuzumab-resistance and metastasis in HER2-positive breast cancers by targeting PTEN. *BMB Rep* 2014;47:268-73.
28. Zhao JJ, Chu ZB, Hu Y, Lin J, Wang Z, Jiang M, et al. Targeting the miR-221-222/PUMA/BAK/BAX Pathway Abrogates Dexamethasone Resistance in Multiple Myeloma. *Cancer Res* 2015;75:4384-97.
29. Ergun S, Arman K, Temiz E, Bozgeyik I, Yumrutas O, Safdar M, et al. Expression patterns of miR-221 and its target Caspase-3 in different cancer cell lines. *Mol Biol Rep* 2014;41:5877-81.
30. Sharma AD, Narain N, Handel EM, Iken M, Singhal N, Cathomen T, et al. MicroRNA-221 regulates FAS-induced fulminant liver failure. *Hepatology* 2011;53:1651-61.
31. Terasawa K, Ichimura A, Sato F, Shimizu K, Tsujimoto G. Sustained activation of ERK1/2 by NGF induces microRNA-221 and 222 in PC12 cells. *FEBS J* 2009;276:3269-76.

Figure Legends.

Figure 1. MiR-221 correlates with Sorafenib resistance in HCC animal models. (A) QPCR analysis of miR-221 expression in 16 DEN-treated rats and two healthy controls (Ctrl). Each nodule was compared with the surrounding liver parenchyma (NL). Y-axis reports the $2^{-\Delta\Delta Ct}$ values corresponding to miR-221 expression. (B, C) Box plot graphic representation of miR-221 and *EPCAM* mRNA expression in DEN-treated rats following 21 days of Sorafenib administration ('Rat + Sorafenib'). HCC nodules were divided in responders (R) and non-responders (NR) based on US imaging and histopathologic examination. Y-axis reports the $2^{-\Delta\Delta Ct}$ values corresponding to gene expression (log2 form). (D, E) Box plot graphic representation of tumor size or tumor doubling time in Sorafenib treated or untreated xenograft mice obtained following subcutaneous injection of Huh-7 cells into the flank of nude mice ('xenograft'). The treated group received Sorafenib intragastrically for 21 days; the untreated group received only the vehicle. Y-axis represents tumor size (mm³) or tumor doubling time (days). (F) Correlation graph between tumor size and miR-221 expression in Sorafenib treated xenograft mice. The xenograft model was obtained by subcutaneous injection of Huh-7 cells and, once the tumors reached a volume of 40-50 mm³, mice received Sorafenib intragastrically for 21 days ('xenograft + Sorafenib'). X-axis reports the $2^{-\Delta\Delta Ct}$ values corresponding to miR-221; y-axis represents tumor size (mm³). All values are transformed in a log2 form.

Figure 2. Circulating miR-221 levels in HCC animal models treated with Sorafenib. (A) Correlation between extracellular and intracellular miR-221 levels in the DEN-HCC rat model (N=13). X and Y-axes report the $2^{-\Delta\Delta Ct}$ values corresponding to intra-tumor and circulating miR-221 levels. (B) Correlation between extracellular and intracellular miR-221 levels in the xenograft model (N=9). X and Y-axes report the $2^{-\Delta\Delta Ct}$ values corresponding to intra-tumor and

circulating miR-221 levels. (C) Negative correlation between extracellular and intracellular miR-221 levels in the DEN-HCC rat model treated by Sorafenib (N=7). X and Y-axes report the $2^{-\Delta\Delta Ct}$ values corresponding to intra-tumor and circulating miR-221 levels. (D, E) Negative correlation between extracellular and intracellular miR-221 levels or tumor size in Sorafenib treated xenograft model (N=5). X-axes reports the $2^{-\Delta\Delta Ct}$ values corresponding to miR-221 intra-tumor levels or tumor size (mm³), respectively. Y-axes report the $2^{-\Delta\Delta Ct}$ values corresponding to circulating miR-221 levels. (F-H) Box plot graph of miR-221 expression in cell culture supernatant, exosomal and intracellular fractions of Sorafenib treated and untreated cell lines. Y-axes report the $2^{-\Delta\Delta Ct}$ values corresponding to miR-221 expression. (A-H) All values are transformed in a log2 form. (I) Circulating miR-221 levels in cell culture supernatant of HCC cells treated with Sorafenib or vehicle (Ctrl) for 48 hours. (L) Circulating miR-221 levels in cell culture supernatant of HCC cells treated with PI3K inhibitor (GDC-0941) or vehicle (Ctrl) for 48 hours. (I, L) Y-axes report the $2^{-\Delta\Delta Ct}$ values corresponding to miR-221 expression. Cel-miR-39 was used to normalize QPCR data. Western blot analysis of pAkt in HepG2, SNU449 and SNU475 in the same settings. β -actin was used to normalize WB data. * p<0.05; ** p<0.01; *** p<0.001.

Figure 3. Circulating miR-221 in patients with advanced HCC treated with Sorafenib. (A) Basal miR-221 levels in patients responding or non-responding to Sorafenib treatment, as assessed at the two months CT/MR examination, in the training set. (B) Circulating miR-221 levels assessed before Sorafenib start and at the two months follow up in patients responding to Sorafenib in the training set. (C) Circulating miR-221 levels in patients responding or non-responding to Sorafenib, as assessed at the two months CT/MR examination, in the validation set. (D) Circulating miR-221 levels assessed before Sorafenib start and at the two months follow up in patients responding to Sorafenib in the validation set. (A, C) Unpaired Student's t-test was

considered for statistical analysis. (B, D) Paired Student's t-test was considered for statistical analysis. (A-D) RNU6B was used as housekeeping gene for QPCR analysis. Y-axes report $2^{-\Delta\Delta Ct}$ values corresponding to circulating miR-221 levels. Pre-treatment: circulating miR-221 levels were evaluated in sera samples collected before treatment. On-treatment: circulating miR-221 levels were evaluated in sera samples collected at two months CT/MR assessment.

Figure 4. MiR-221 decreases Sorafenib activity in HCC cell lines. (A, B) Cell viability assay, caspase 3/7 activity assay and Western blot analysis in transient miR-221 over-expressing Huh-7 and Hep3B cells subjected to Sorafenib. (C) Cell viability assay, caspase 3/7 activity assay and Western blot analysis in Huh-7 cells stably infected with pMXs-miR-221 over-expression vector subjected to Sorafenib treatment. (D, E) Cell viability assay, caspase 3/7 activity assay and Western blot analysis in transient miR-221 silenced SNU182 and SNU449 cells following Sorafenib treatment. (F) Annexin V cytofluorimetric analysis in miR-221 stably over-expressing Huh-7 cells subjected to Sorafenib treatment. (A-F) NC: pre-miR negative control; NCi: anti-miR negative control; AM-221: anti-miR-221; shRNA: scramble short hairpin RNA control vector. (A-E) β -actin was used to normalize WB data.

Figure 5. MiR-221 targets caspase-3 in HCC. (A) MiR-221 hypothetical binding site in caspase-3 3'UTR as shown by MiRanda and TargetScan algorithms. Stars represent the mutagenized basis in the reporter assay. (B) QPCR and WB analyses of miR-221 and caspase-3 levels in HCC-derived cell lines. Y-axis reports the $2^{-\Delta\Delta Ct}$ values corresponding to miR-221 or caspase-3 mRNA levels. Correlation graphs represent the relationship between miR-221 and caspase-3 mRNA and protein levels. All the values are in a log2 form. (C) Western blot, RT-PCR and QPCR analyses in miR-221 over-expressing HepG2 cells. (D, E) Western blot, RT-

PCR and QPCR analyses in transient and stable miR-221 over-expressing Huh-7 cells. **(F, G)** Western blot, RT-PCR and QPCR analyses in miR-221 silenced SNU449 and SNU182 cells. **(B-G)** β -actin was used to normalize PCR and WB data. **(C-G)** Bar charts below WB images display mean \pm SD values relative to immunoblot quantification of three different replicates. Bar charts below RT-PCR images represent mean \pm SD values relative to QPCR analysis. **(H)** Luciferase reporter assay in HepG2 and SNU449 cells co-transfected with WT or mutated pGL3-casp3 vector and miR-221 or AM-221. **(I)** Western blot analysis of apoptotic markers in co-transfected SNU449 cells subjected to Sorafenib treatment. β -actin was used as housekeeping gene. **(C-I)** pGL3: empty reporter vector; NC: pre-miR negative control; NCi: anti-miR negative control; AM: anti-miR-221; shRNA: scramble short hairpin RNA control vector; scr: scramble oligonucleotides; si: small interfering RNAs.

Figure 6. MiR-221 targets caspase-3 in vivo. **(A)** Western blot analysis of caspase-3 expression in miR-221 liver-specific transgenic (TG) and wild type (WT) mice (representative cases). β -actin was used as housekeeping gene. Numbers represent the densitometric analysis of WB bands normalized for the housekeeping gene. The bar chart below WB image displays mean \pm SD values relative to immunoblot quantification of three different replicates. **(B)** Box plot graph of caspase-3 expression in TG and WT mice. Y-axis reports the $2^{-\Delta\Delta C_t}$ values corresponding to caspase-3 expression. **(C)** Western blot and QPCR analyses of caspase-3 and miR-221 expression in TG mice treated with anti-miR-221 oligonucleotides (AM-221) or with vehicle (representative cases). **(D)** Western blot and QPCR analyses of caspase-3 and miR-221 expression in TG mice treated with anti-miR-221 oligonucleotides (AM-221) or with vehicle and subjected to Sorafenib administration. (C, D) β -actin was used as housekeeping gene. Numbers represent the densitometric analysis of WB bands normalized for the housekeeping gene. The bar charts below WB images display mean \pm SD values of caspase-3 expression in the two mice

groups. (**E, F**) Negative correlation between miR-221 expression and caspase-3 mRNA (N=24) or caspase-3 protein (N=23) levels in the DEN-HCCs. X and Y-axes report the $2^{-\Delta\Delta C_t}$ values corresponding to miR-221 levels and caspase-3 mRNA or protein levels (log2 form). (**G**) Negative correlation between miR-221 expression and caspase-3 mRNA (N=60) levels in human HCCs. X and Y-axes report the $2^{-\Delta\Delta C_t}$ values corresponding to miR-221 and caspase-3 mRNA levels (log2 form). (**H, I**) Box plot graph of miR-221 and caspase-3 expression in unifocal (UNI) and multifocal (MULTI) human HCCs. Y-axis reports the $2^{-\Delta\Delta C_t}$ values corresponding to miR-221 or caspase-3 expression (log2 form). B-actin was used for WB and QPCR normalization.

Figure 1

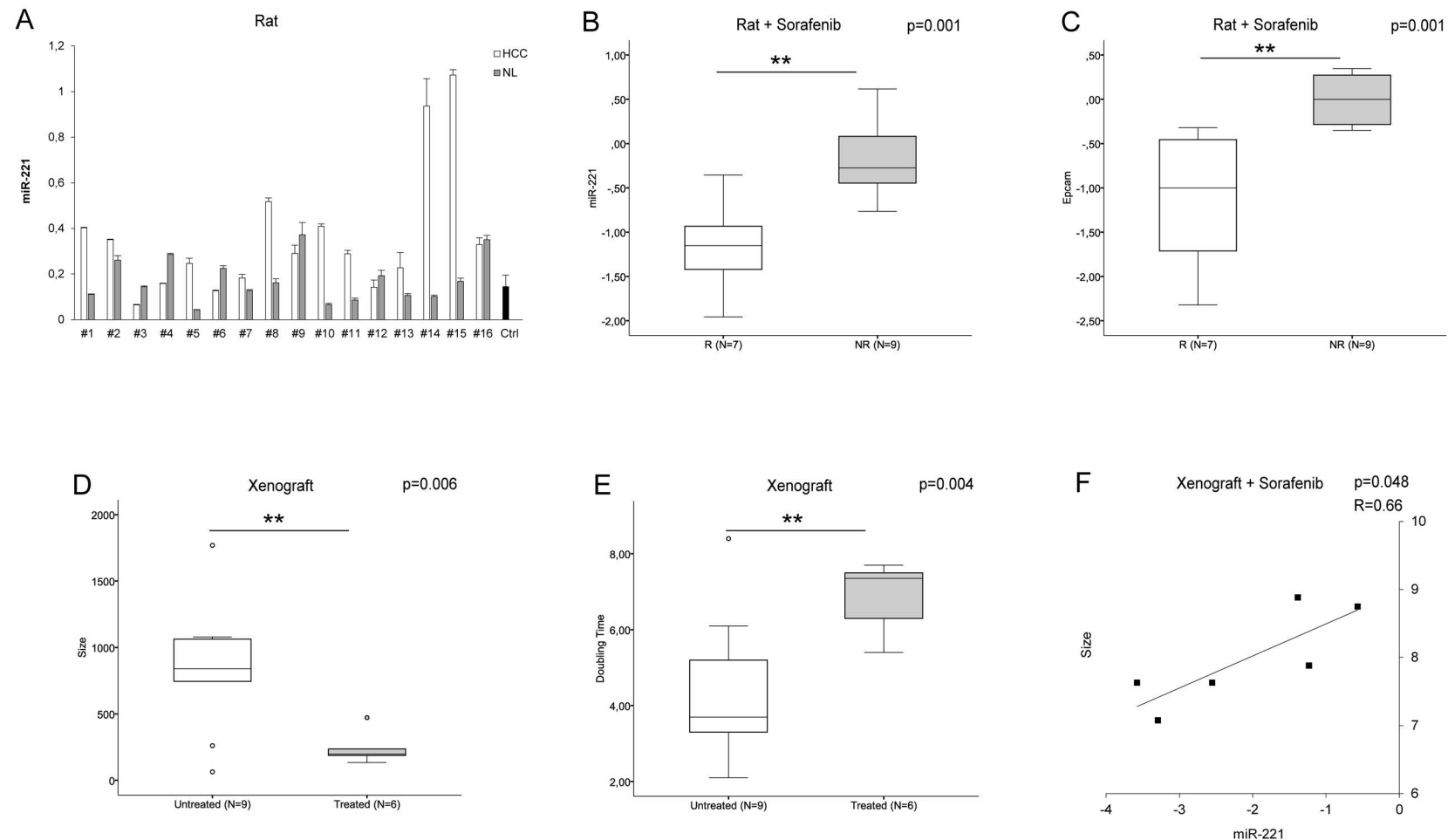


Figure 2

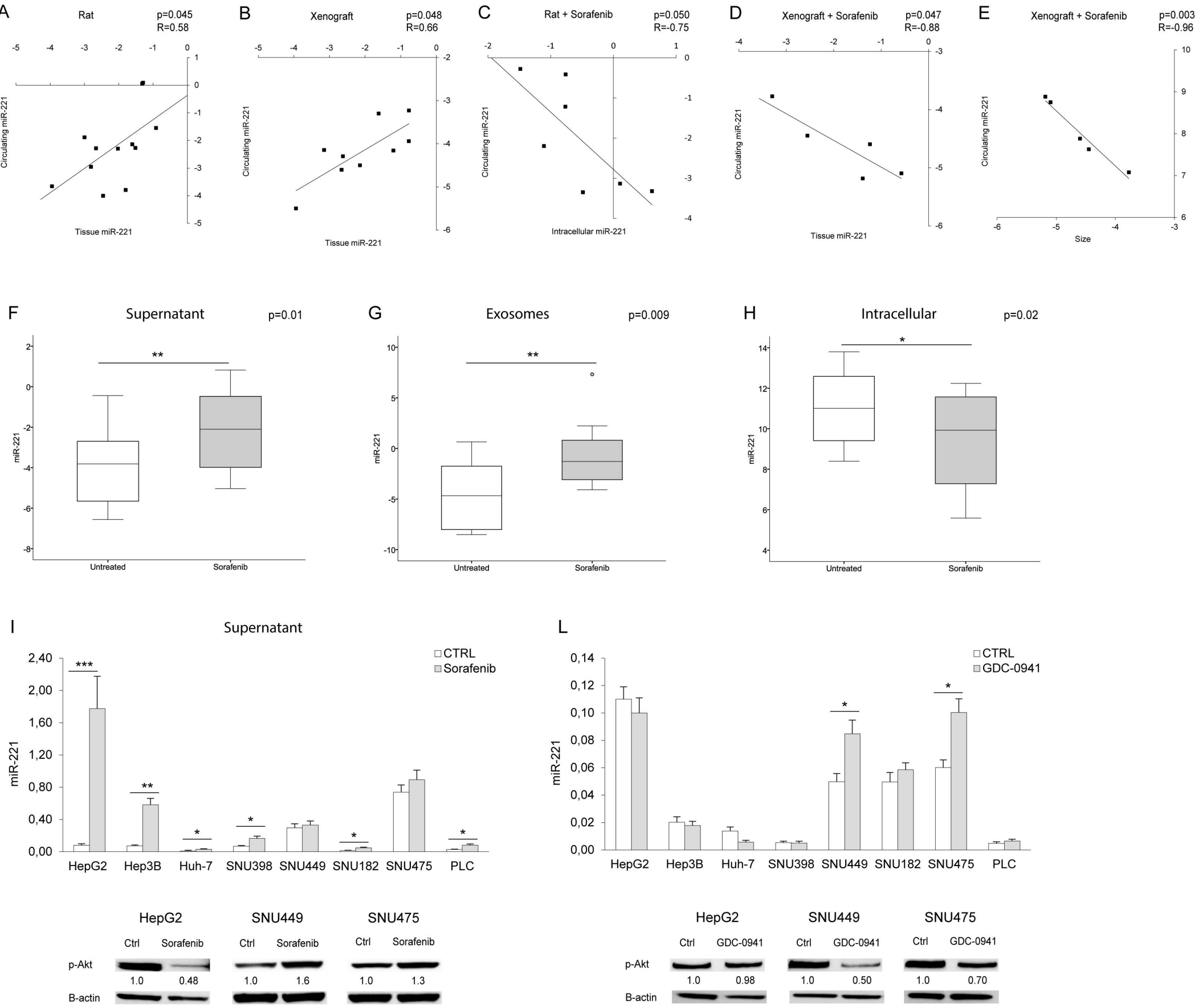


Figure 3

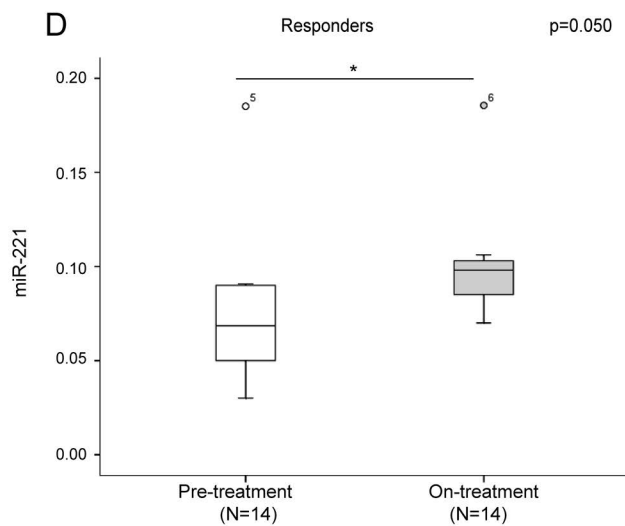
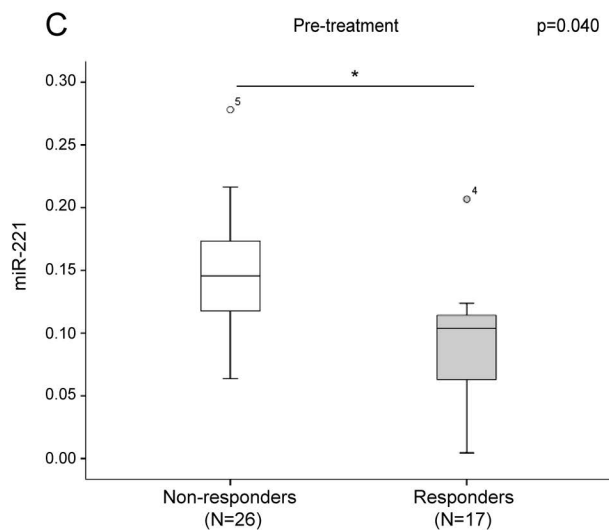
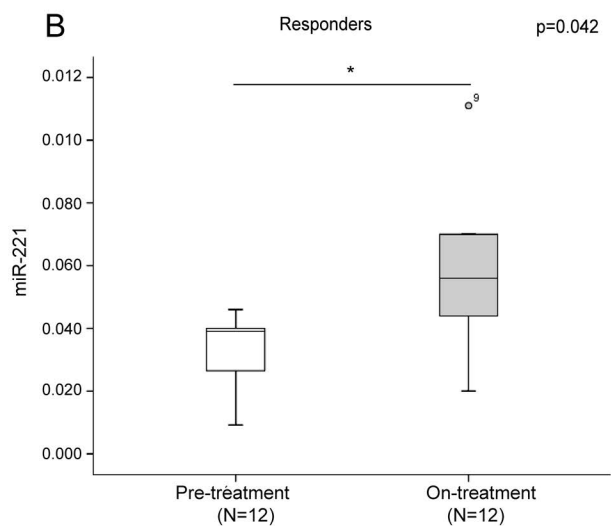
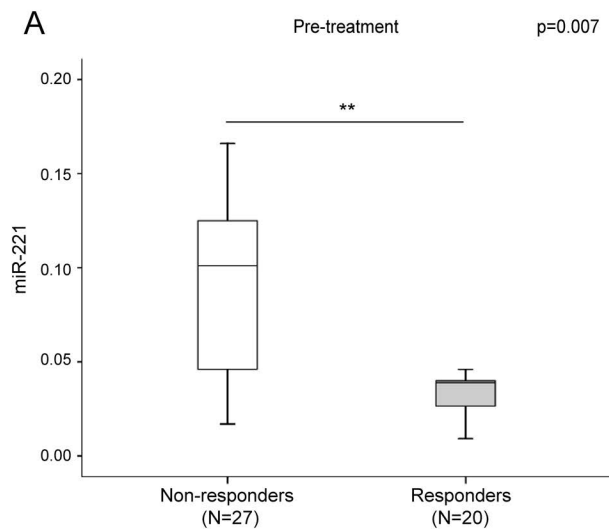
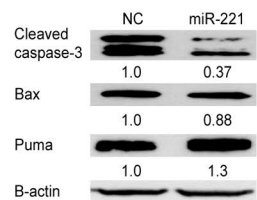
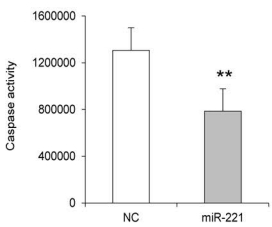
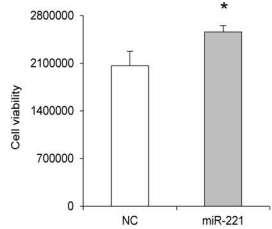
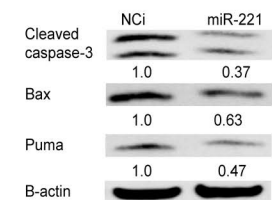
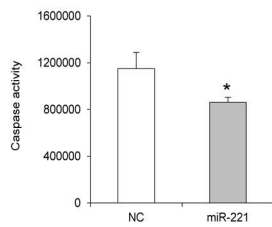
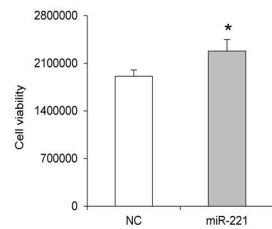


Figure 4

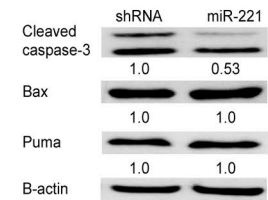
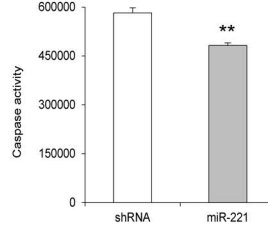
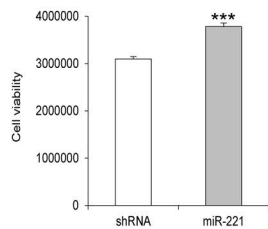
A Transient Huh-7 + Sorafenib



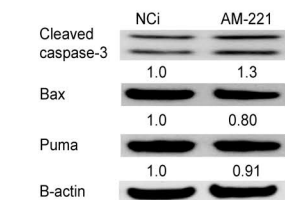
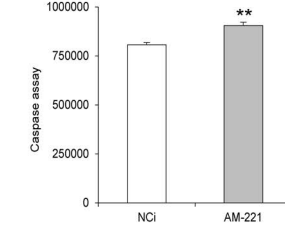
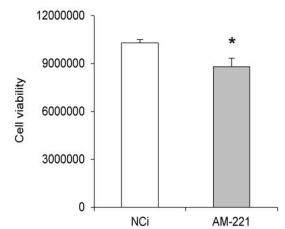
B Hep3B + Sorafenib



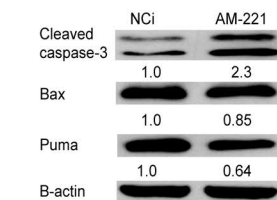
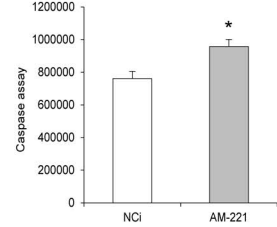
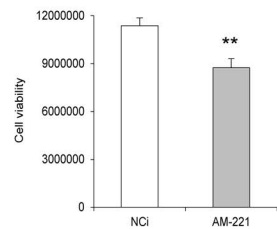
C Stable Huh-7 + Sorafenib



D SNU182 + Sorafenib



E SNU449 + Sorafenib



F

Huh-7 + Sorafenib

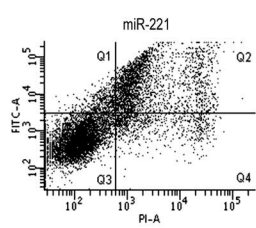
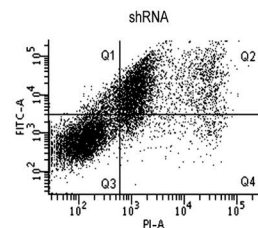


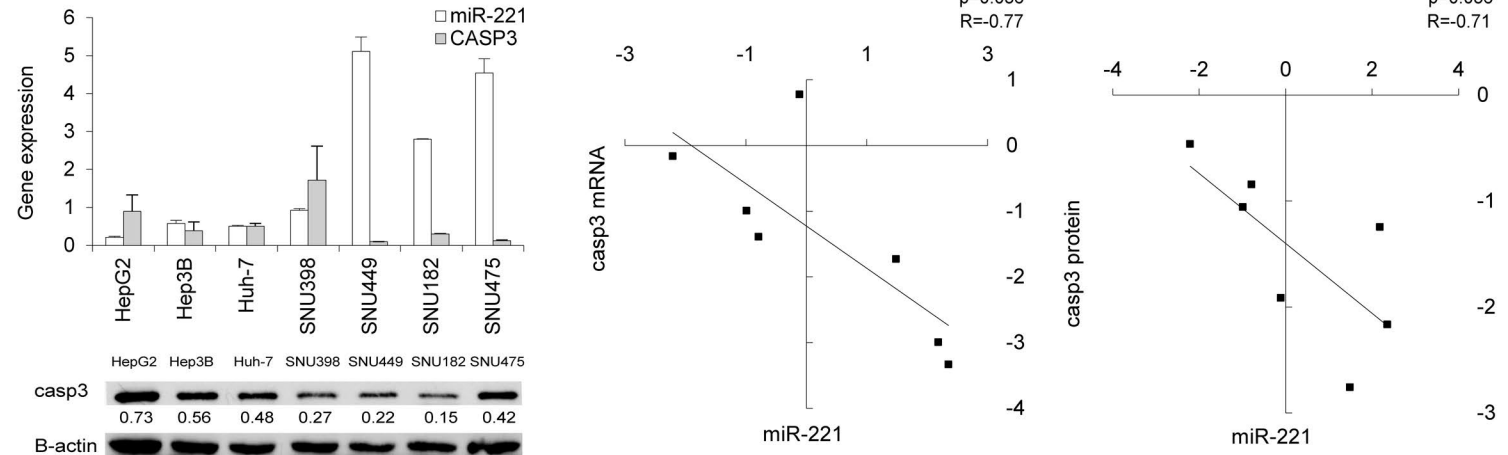
Figure 5

A

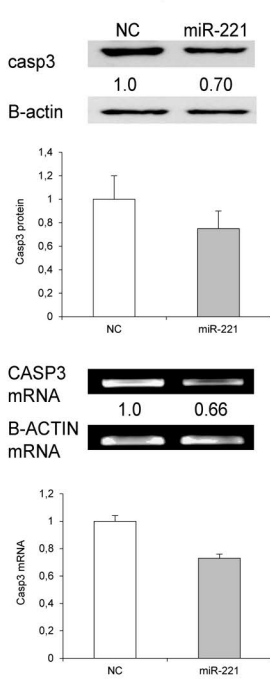
hsa-miR-221/CASP3 Alignment	
3' cuUUGG-GUCGUCUGUUAUCAUGa 5' hsa-miR-221 : :	mirSVR score: -0.1455 PhastCons score: 0.5557
1134:5' aaAAUCAUAAGUACUCUUUGUAGCa 3' CASP3 ***** CASP3-MUT	

	predicted consequential pairing of target region (top) and miRNA (bottom)	seed match	context+ score
Position 1151-1157 of CASP3 3' UTR	5' ... AAUCAUAAGUACUCUU-UGUAGCA... 3' ...	7mer-1A	-0.16
Position 1151-1157 of CASP3 3' UTR	5' ... AAUCAUAAGUACUCUUUGUAGCA... 3' ...	7mer-1A	-0.15

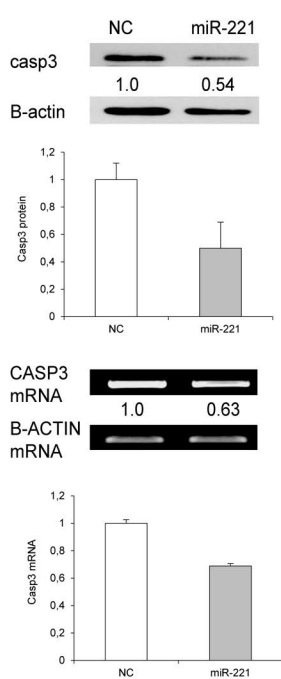
B



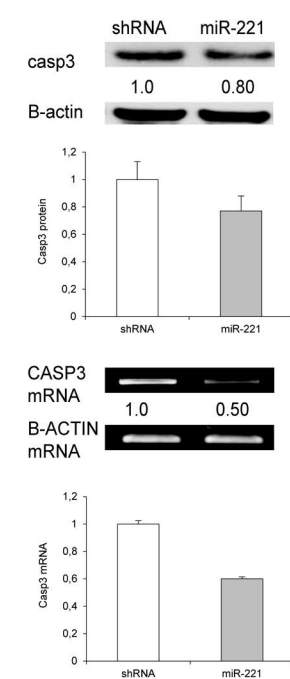
C



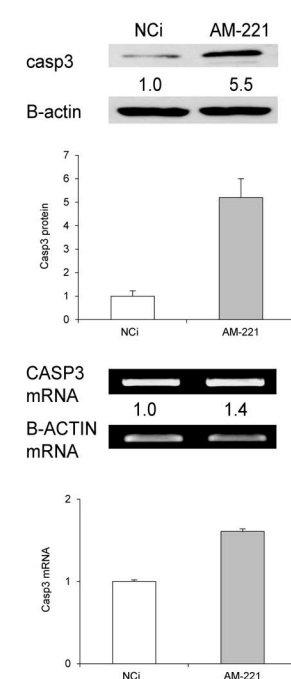
D



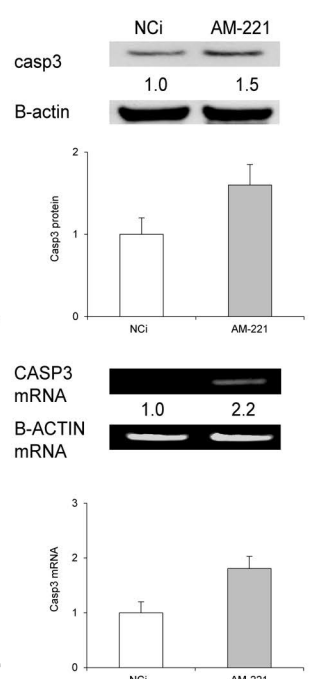
E



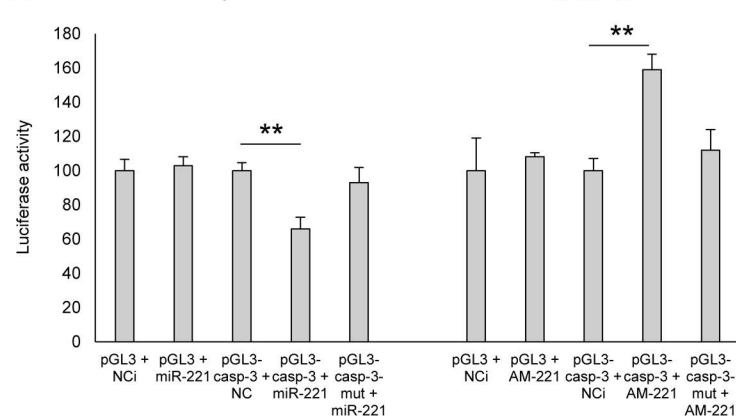
F



G



H



I

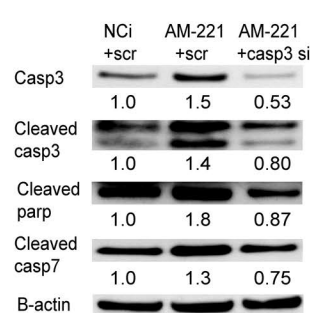


Figure 6

